Determination of the Pseudoscalar Decay Constant $f_{D_s^+}$ via $D_s^+ \to \mu^+ \nu_\mu$

M. Ablikim,[1] M. N. Achasov,[9,d] S. Ahmed,[14] M. Albrecht,[4] M. Alekseev,[56a,56c] A. Amoroso,[56a,56c] F. F. An,[1] Q. An,[53,43] Y. Bai,[42] O. Bakina,[26] R. Baldini Ferroli,[22a] Y. Ban,[34] K. Begzsuren,[24] D. W. Bennett,[21] J. V. Bennett,[5] N. Berger,[25] M. Bertani,[22a] D. Bettoni,[23a] F. Bianchi,[56a,56c] I. Boyko,[26] R. A. Briere,[5] H. Cai,[58] X. Cai,[1,43] O. Cakir,[46a] A. Calcaterra,[22a] G. F. Cao,[1,47] S. A. Cetin,[46b] J. Chai,[56c] J. F. Chang,[1,43] W. L. Chang,[1,47] G. Chelkov,[26,b,c] G. Chen,[1] H. S. Chen,[1,47] J. C. Chen,[1] M. L. Chen,[1,43] P. L. Chen,[54] S. J. Chen,[32] Y. B. Chen,[1,43] G. Cibinetto,[23a] F. Cossio,[56c] H. L. Dai,[1,43] J. P. Dai,[38,h] A. Dbeyssi,[14] D. Dedovich,[26] Z. Y. Deng,[1] A. Denig,[25] I. Denysenko,[26] M. Destefanis,[56a,56c] F. De Mori,[56a,56c] Y. Ding,[30] C. Dong,[33] J. Dong,[1,43] L. Y. Dong,[1,47] M. Y. Dong,[1,43,47] Z. L. Dou,[32] S. X. Du,[61] P. F. Duan,[1] J. Z. Fan,[45] J. Fang,[1,43] S. S. Fang,[1,47] Y. Fang,[1] R. Farinelli,[23a,23b] L. Fava,[56b,56c] S. Fegan,[25] F. Feldbauer,[4] G. Felici,[22a] C. Q. Feng,[53,43] M. Fritsch,[4] C. D. Fu,[1] Y. Fu,[1] Q. Gao,[1] X. L. Gao,[53,43] Y. Gao,[45] Y. G. Gao,[6] Z. Gao,[53,43] B. Garillon,[25] I. Garzia,[23a] A. Gilman,[50] K. Goetzen,[10] L. Gong,[33] W. X. Gong,[1,43] W. Gradl,[25] M. Greco,[56a,56c] L. M. Gu,[32] M. H. Gu,[1,43] Y. T. Gu,[12] A. Q. Guo,[1] L. B. Guo,[31] R. P. Guo,[36] Y. P. Guo,[25] A. Guskov,[26] Z. Haddadi,[28] S. Han,[58] X. Q. Hao,[15] F. A. Harris,[48] K. L. He,[1,47] F. H. Heinsius,[4] T. Held,[4] Y. K. Heng,[1,43,47] T. Holtmann,[4] Z. L. Hou,[1] H. M. Hu,[1,47] J. F. Hu,[38,h] T. Hu,[1,43,47] Y. Hu,[1] G. S. Huang,[53,43] J. S. Huang,[15] X. T. Huang,[37] X. Z. Huang,[32] Z. L. Huang,[30] T. Hussain,[55] W. Ikegami Andersson,[57] M. Irshad,[53,43] Q. Ji,[1] Q. P. Ji,[15] X. B. Ji,[1,47] X. L. Ji,[1,43] X. S. Jiang,[1,43,47] X. Y. Jiang,[33] J. B. Jiao,[37] Z. Jiao,[17] D. P. Jin,[1,43,47] S. Jin,[32] Y. Jin,[49] T. Johansson,[57] A. Julin,[50] N. Kalantar-Nayestanaki,[28] X. S. Kang,[33] M. Kavatsyuk,[28] B. C. Ke,[1] T. Khan,[53,43] A. Khoukaz,[51] P. Kiese,[25] R. Kliemt,[10] L. Koch,[27] O. B. Kolcu,[46b,f] B. Kopf,[4] M. Kornicer,[48] M. Kuemmel,[4] M. Kuessner,[4] A. Kupsc,[57] M. Kurth,[1] W. Kühn,[27] J. S. Lange,[27] M. Lara,[21] P. Larin,[14] L. Lavezzi,[56c] S. Leiber,[4] H. Leithoff,[25] C. Li,[57] Cheng Li,[53,43] D. M. Li,[61] F. Li,[1,43] F. Y. Li,[34] G. Li,[1] H. B. Li,[1,47] H. J. Li,[1,47] J. C. Li,[1] J. W. Li,[41] Ke Li,[1] Lei Li,[3] P. L. Li,[53,43] P. R. Li,[47,7] Q. Y. Li,[37] T. Li,[37] W. D. Li,[1,47] W. G. Li,[1] X. L. Li,[37] X. N. Li,[1,43] X. Q. Li,[33] Z. B. Li,[44] H. Liang,[53,43] Y. F. Liang,[40] Y. T. Liang,[27] G. R. Liao,[11] L. Z. Liao,[1,47] J. Libby,[20] C. X. Lin,[44] D. X. Lin,[14] B. Liu,[38,h] B. J. Liu,[1] C. X. Liu,[1] D. Liu,[53,43] D. Y. Liu,[38,h] F. H. Liu,[39] Fang Liu,[1] Feng Liu,[6] H. B. Liu,[12] H. L. Liu,[42] H. M. Liu,[1,47] Huanhuan Liu,[1] Huihui Liu,[16] J. B. Liu,[53,43] J. Y. Liu,[1,47] K. Liu,[45] K. Y. Liu,[30] Ke Liu,[6] Q. Liu,[47] S. B. Liu,[53,43] X. Liu,[29] Y. B. Liu,[33] Z. A. Liu,[1,43,47] Zhiqing Liu,[25] Y. F. Long,[34] X. C. Lou,[1,43,47] H. J. Lu,[17] J. D. Lu,[1,47] J. G. Lu,[1,43] Y. Lu,[1] Y. P. Lu,[1,43] C. L. Luo,[31] M. X. Luo,[60] X. L. Luo,[1,43] S. Lusso,[56c] X. R. Lyu,[47] F. C. Ma,[30] H. L. Ma,[1] L. L. Ma,[37] M. M. Ma,[1,47] Q. M. Ma,[1] X. N. Ma,[33] X. X. Ma,[1,47] X. Y. Ma,[1,43] Y. M. Ma,[37] F. E. Maas,[14] M. Maggiora,[56a,56c] Q. A. Malik,[55] A. Mangoni,[22b] Y. J. Mao,[34] Z. P. Mao,[1] S. Marcello,[56a,56c] Z. X. Meng,[49] J. G. Messchendorp,[28] G. Mezzadri,[23a] J. Min,[1,43] T. J. Min,[32] R. E. Mitchell,[21] X. H. Mo,[1,43,47] Y. J. Mo,[6] C. Morales Morales,[14] G. Morello,[22a] N. Yu. Muchnoi,[9,d] H. Muramatsu,[50] A. Mustafa,[4] S. Nakhoul,[10,g] Y. Nefedov,[26] F. Nerling,[10,g] I. B. Nikolaev,[9,d] Z. Ning,[1,43] S. Nisar,[8,k] S. L. Niu,[1,43] S. L. Olsen,[35,j] Q. Ouyang,[1,43,47] S. Pacetti,[22b] Y. Pan,[53,43] M. Papenbrock,[57] P. Patteri,[22a] M. Pelizaeus,[4] J. Pellegrino,[56a,56c] H. P. Peng,[53,43] K. Peters,[10,g] J. Pettersson,[57] J. L. Ping,[31] R. G. Ping,[1,47] A. Pitka,[4] R. Poling,[50] V. Prasad,[53,43] H. R. Qi,[2] M. Qi,[32] T. Y. Qi,[2] S. Qian,[1,43] C. F. Qiao,[47] N. Qin,[58] X. S. Qin,[4] Z. H. Qin,[1,43] J. F. Qiu,[1] K. H. Rashid,[55,i] C. F. Redmer,[25] M. Richter,[4] M. Ripka,[25] M. Rolo,[56c] G. Rong,[1,47] Ch. Rosner,[14] A. Sarantsev,[26,e] M. Savrié,[23b] C. Schnier,[4] K. Schoenning,[57] W. Shan,[18] X. Y. Shan,[53,43] M. Shao,[53,43] C. P. Shen,[2] P. X. Shen,[33] X. Y. Shen,[1,47] H. Y. Sheng,[1] X. Shi,[1,43] J. J. Song,[37] W. M. Song,[37] X. Y. Song,[1] S. Sosio,[56a,56c] C. Sowa,[4] S. Spataro,[56a,56c] G. X. Sun,[1] J. F. Sun,[15] L. Sun,[58] S. S. Sun,[1,47] X. H. Sun,[1] Y. J. Sun,[53,43] Y. K. Sun,[53,43] Y. Z. Sun,[1] Z. J. Sun,[1,43] Z. T. Sun,[21] Y. T. Tan,[53,43] C. J. Tang,[40] G. Y. Tang,[1] X. Tang,[1] I. Tapan,[46c] M. Tiemens,[28] B. Tsednee,[24] I. Uman,[46d] G. S. Varner,[48] B. Wang,[1] B. L. Wang,[47] C. W. Wang,[32] D. Y. Wang,[34] Dan Wang,[47] K. Wang,[1,43] L. L. Wang,[1] L. S. Wang,[1] M. Wang,[37] Meng Wang,[1,47] P. Wang,[1] P. L. Wang,[1] W. P. Wang,[53,43] X. F. Wang,[1] Y. Wang,[53,43] Y. F. Wang,[1,43,47] Y. Q. Wang,[25] Z. Wang,[1,43] Z. G. Wang,[1,43] Z. Y. Wang,[1] Zongyuan Wang,[1,47] T. Weber,[4] D. H. Wei,[11] P. Weidenkaff,[25] S. P. Wen,[1] U. Wiedner,[4] M. Wolke,[57] L. H. Wu,[1] L. J. Wu,[1,47] Z. Wu,[1,43] L. Xia,[53,43] X. Xia,[37] Y. Xia,[19] D. Xiao,[1] Y. J. Xiao,[1,47] Z. J. Xiao,[31] Y. G. Xie,[1,43] Y. H. Xie,[6] X. A. Xiong,[1,47] Q. L. Xiu,[1,43] G. F. Xu,[1] J. J. Xu,[1,47] L. Xu,[1] Q. J. Xu,[13] Q. N. Xu,[47] X. P. Xu,[41] F. Yan,[54] L. Yan,[56a,56c] W. B. Yan,[53,43] W. C. Yan,[2] Y. H. Yan,[19] H. J. Yang,[38,h] H. X. Yang,[1] L. Yang,[58] S. L. Yang,[1,47] Y. H. Yang,[32] Y. X. Yang,[11] Yifan Yang,[1,47] M. Ye,[1,43] M. H. Ye,[7] J. H. Yin,[1] Z. Y. You,[44] B. X. Yu,[1,43,47] C. X. Yu,[33] C. Z. Yuan,[1,47] Y. Yuan,[1] A. Yuncu,[46b,a] A. A. Zafar,[55] A. Zallo,[22a] Y. Zeng,[19] Z. Zeng,[53,43] B. X. Zhang,[1] B. Y. Zhang,[1,43] C. C. Zhang,[1] D. H. Zhang,[1] H. H. Zhang,[44] H. Y. Zhang,[1,43] J. Zhang,[1,47] J. L. Zhang,[59] J. Q. Zhang,[4] J. W. Zhang,[1,43,47] J. Y. Zhang,[1] J. Z. Zhang,[1,47] K. Zhang,[1,47] L. Zhang,[45] S. F. Zhang,[32] T. J. Zhang,[38,h] X. Y. Zhang,[37] Y. Zhang,[53,43] Y. H. Zhang,[1,43] Y. T. Zhang,[53,43] Yang Zhang,[1] Yao Zhang,[1] Yu Zhang,[47] Z. H. Zhang,[6] Z. P. Zhang,[53] Z. Y. Zhang,[58] G. Zhao,[1] J. W. Zhao,[1,43] J. Y. Zhao,[1,47] J. Z. Zhao,[1,43] Lei Zhao,[53,43] Ling Zhao,[1] M. G. Zhao,[33] Q. Zhao,[1] S. J. Zhao,[61] T. C. Zhao,[1] Y. B. Zhao,[1,43] Z. G. Zhao,[53,43] A. Zhemchugov,[26,b] B. Zheng,[54] J. P. Zheng,[1,43] W. J. Zheng,[37] Y. H. Zheng,[47] B. Zhong,[31] L. Zhou,[1,43] Q. Zhou,[1,47] X. Zhou,[58] X. K. Zhou,[53,43] X. R. Zhou,[53,43] X. Y. Zhou,[1] A. N. Zhu,[1,47] J. Zhu,[33] J. Zhu,[44] K. Zhu,[1] K. J. Zhu,[1,43,47] S. Zhu,[1] S. H. Zhu,[52] X. L. Zhu,[45] Y. C. Zhu,[53,43] Y. S. Zhu,[1,47] Z. A. Zhu,[1,47] J. Zhuang,[1,43] B. S. Zou,[1] and J. H. Zou[1]

(BESIII Collaboration)

[1]*Institute of High Energy Physics, Beijing 100049, People's Republic of China*
[2]*Beihang University, Beijing 100191, People's Republic of China*
[3]*Beijing Institute of Petrochemical Technology, Beijing 102617, People's Republic of China*
[4]*Bochum Ruhr-University, D-44780 Bochum, Germany*
[5]*Carnegie Mellon University, Pittsburgh, Pennsylvania 15213, USA*
[6]*Central China Normal University, Wuhan 430079, People's Republic of China*
[7]*China Center of Advanced Science and Technology, Beijing 100190, People's Republic of China*
[8]*COMSATS University Islamabad, Lahore Campus, Defence Road, Off Raiwind Road, 54000 Lahore, Pakistan*
[9]*G.I. Budker Institute of Nuclear Physics SB RAS (BINP), Novosibirsk 630090, Russia*
[10]*GSI Helmholtzcentre for Heavy Ion Research GmbH, D-64291 Darmstadt, Germany*
[11]*Guangxi Normal University, Guilin 541004, People's Republic of China*
[12]*Guangxi University, Nanning 530004, People's Republic of China*
[13]*Hangzhou Normal University, Hangzhou 310036, People's Republic of China*
[14]*Helmholtz Institute Mainz, Johann-Joachim-Becher-Weg 45, D-55099 Mainz, Germany*
[15]*Henan Normal University, Xinxiang 453007, People's Republic of China*
[16]*Henan University of Science and Technology, Luoyang 471003, People's Republic of China*
[17]*Huangshan College, Huangshan 245000, People's Republic of China*
[18]*Hunan Normal University, Changsha 410081, People's Republic of China*
[19]*Hunan University, Changsha 410082, People's Republic of China*
[20]*Indian Institute of Technology Madras, Chennai 600036, India*
[21]*Indiana University, Bloomington, Indiana 47405, USA*
[22a]*INFN Laboratori Nazionali di Frascati, I-00044, Frascati, Italy*
[22b]*INFN and University of Perugia, I-06100, Perugia, Italy*
[23a]*INFN Sezione di Ferrara, I-44122, Ferrara, Italy*
[23b]*University of Ferrara, I-44122, Ferrara, Italy*
[24]*Institute of Physics and Technology, Peace Ave. 54B, Ulaanbaatar 13330, Mongolia*
[25]*Johannes Gutenberg University of Mainz, Johann-Joachim-Becher-Weg 45, D-55099 Mainz, Germany*
[26]*Joint Institute for Nuclear Research, 141980 Dubna, Moscow region, Russia*
[27]*Justus-Liebig-Universitaet Giessen, II. Physikalisches Institut, Heinrich-Buff-Ring 16, D-35392 Giessen, Germany*
[28]*KVI-CART, University of Groningen, NL-9747 AA Groningen, Netherlands*
[29]*Lanzhou University, Lanzhou 730000, People's Republic of China*
[30]*Liaoning University, Shenyang 110036, People's Republic of China*
[31]*Nanjing Normal University, Nanjing 210023, People's Republic of China*
[32]*Nanjing University, Nanjing 210093, People's Republic of China*
[33]*Nankai University, Tianjin 300071, People's Republic of China*
[34]*Peking University, Beijing 100871, People's Republic of China*
[35]*Seoul National University, Seoul, 151-747 Korea*
[36]*Shandong Normal University, Jinan 250014, People's Republic of China*
[37]*Shandong University, Jinan 250100, People's Republic of China*
[38]*Shanghai Jiao Tong University, Shanghai 200240, People's Republic of China*
[39]*Shanxi University, Taiyuan 030006, People's Republic of China*
[40]*Sichuan University, Chengdu 610064, People's Republic of China*
[41]*Soochow University, Suzhou 215006, People's Republic of China*
[42]*Southeast University, Nanjing 211100, People's Republic of China*
[43]*State Key Laboratory of Particle Detection and Electronics, Beijing 100049, Hefei 230026, People's Republic of China*
[44]*Sun Yat-Sen University, Guangzhou 510275, People's Republic of China*
[45]*Tsinghua University, Beijing 100084, People's Republic of China*
[46a]*Ankara University, 06100 Tandogan, Ankara, Turkey*
[46b]*Istanbul Bilgi University, 34060 Eyup, Istanbul, Turkey*
[46c]*Uludag University, 16059 Bursa, Turkey*
[46d]*Near East University, Nicosia, North Cyprus, Mersin 10, Turkey*
[47]*University of Chinese Academy of Sciences, Beijing 100049, People's Republic of China*

[48]University of Hawaii, Honolulu, Hawaii 96822, USA
[49]University of Jinan, Jinan 250022, People's Republic of China
[50]University of Minnesota, Minneapolis, Minnesota 55455, USA
[51]University of Muenster, Wilhelm-Klemm-Str. 9, 48149 Muenster, Germany
[52]University of Science and Technology Liaoning, Anshan 114051, People's Republic of China
[53]University of Science and Technology of China, Hefei 230026, People's Republic of China
[54]University of South China, Hengyang 421001, People's Republic of China
[55]University of the Punjab, Lahore-54590, Pakistan
[56a]University of Turin, I-10125, Turin, Italy
[56b]University of Eastern Piedmont, I-15121, Alessandria, Italy
[56c]INFN, I-10125, Turin, Italy
[57]Uppsala University, Box 516, SE-75120 Uppsala, Sweden
[58]Wuhan University, Wuhan 430072, People's Republic of China
[59]Xinyang Normal University, Xinyang 464000, People's Republic of China
[60]Zhejiang University, Hangzhou 310027, People's Republic of China
[61]Zhengzhou University, Zhengzhou 450001, People's Republic of China

(Received 27 November 2018; revised manuscript received 18 January 2019; published 22 February 2019)

Using a 3.19 fb^{-1} data sample collected at an e^+e^- center-of-mass energy of $E_{\mathrm{cm}} = 4.178$ GeV with the BESIII detector, we measure the branching fraction of the leptonic decay $D_s^+ \to \mu^+\nu_\mu$ to be $\mathcal{B}_{D_s^+\to\mu^+\nu_\mu} = (5.49 \pm 0.16_{\mathrm{stat}} \pm 0.15_{\mathrm{syst}}) \times 10^{-3}$. Combining our branching fraction with the masses of the D_s^+ and μ^+ and the lifetime of the D_s^+, we determine $f_{D_s^+}|V_{cs}| = 246.2 \pm 3.6_{\mathrm{stat}} \pm 3.5_{\mathrm{syst}}$ MeV. Using the $c \to s$ quark mixing matrix element $|V_{cs}|$ determined from a global standard model fit, we evaluate the D_s^+ decay constant $f_{D_s^+} = 252.9 \pm 3.7_{\mathrm{stat}} \pm 3.6_{\mathrm{syst}}$ MeV. Alternatively, using the value of $f_{D_s^+}$ calculated by lattice quantum chromodynamics, we find $|V_{cs}| = 0.985 \pm 0.014_{\mathrm{stat}} \pm 0.014_{\mathrm{syst}}$. These values of $\mathcal{B}_{D_s^+\to\mu^+\nu_\mu}$, $f_{D_s^+}|V_{cs}|$, $f_{D_s^+}$ and $|V_{cs}|$ are each the most precise results to date.

DOI: 10.1103/PhysRevLett.122.071802

The leptonic decay $D_s^+ \to \ell^+\nu_\ell$ ($\ell = e$, μ, or τ) offers a unique window into both strong and weak effects in the charm quark sector. In the standard model (SM), the partial width of the decay $D_s^+ \to \ell^+\nu_\ell$ can be written as [1]

$$\Gamma_{D_s^+\to\ell^+\nu_\ell} = \frac{G_F^2}{8\pi}|V_{cs}|^2 f_{D_s^+}^2 m_\ell^2 m_{D_s^+}\left(1 - \frac{m_\ell^2}{m_{D_s^+}^2}\right)^2, \quad (1)$$

where $f_{D_s^+}$ is the D_s^+ decay constant, $|V_{cs}|$ is the $c \to s$ Cabibbo-Kobayashi-Maskawa (CKM) matrix element, G_F is the Fermi coupling constant, m_ℓ is the lepton mass, and $m_{D_s^+}$ is the D_s^+ mass. In recent years, much progress has been achieved in the measurements of $f_{D_s^+}$ and $|V_{cs}|$ with $D_s^+ \to \ell^+\nu_\ell$ decays at the CLEO [2–4], *BABAR* [5], Belle [6] and BESIII [7] experiments. However, compared to the precision of the most accurate lattice quantum chromodynamics (LQCD) calculation of $f_{D_s^+}$ [8], the accuracy of the measurements is still limited. Improved measurements of $f_{D_s^+}$ and $|V_{cs}|$ are critical to calibrate various theoretical calculations of $f_{D_s^+}$ [8–37], such as those from quenched and unquenched LQCD, QCD sum rules, etc., and to test the unitarity of the quark mixing matrix with better precision.

In the SM, the ratio of the branching fraction (BF) of $D_s^+ \to \tau^+\nu_\tau$ over that of $D_s^+ \to \mu^+\nu_\mu$ is predicted to be 9.74 with negligible uncertainty and the BFs of $D_s^+ \to \mu^+\nu_\mu$ and $D_s^- \to \mu^-\bar{\nu}_\mu$ decays are expected to be the same. However, hints of lepton flavor universality (LFU) violation in semileptonic B decays were recently reported at *BABAR*, LHCb, and Belle [38–42]. It has been argued that new physics mechanisms, such as a two-Higgs-doublet model with the mediation of charged Higgs bosons [43,44] or a seesaw mechanism due to lepton mixing with Majorana neutrinos [45], may cause LFU or *CP* violation. Tests of LFU and searches for *CP* violation in $D_s^+ \to \ell^+\nu_\ell$ decays are therefore important tests of the SM.

In this Letter, we present an experimental study of the leptonic decay $D_s^+ \to \mu^+\nu_\mu$ [46] by analyzing a 3.19 fb^{-1} data sample collected with the BESIII detector at an e^+e^- center-of-mass energy of $E_{\mathrm{cm}} = 4.178$ GeV. At this energy, D_s^+ mesons are produced mainly through the process $e^+e^- \to D_s^+ D_s^{*-}$ + c.c. In an event where a D_s^- meson [called a single-tag (ST) D_s^- meson] is fully reconstructed, one can then search for a γ or π^0 and a D_s^+ meson in the recoiling system [called a double-tag (DT) event].

Details about the design and performance of the BESIII detector are given in Ref. [47]. The end cap time-of-flight (TOF) system was upgraded with multigap resistive plate chamber technology and now has a time resolution of 60 ps [48,49]. Monte Carlo (MC) events are generated with a GEANT4-based [50] detector simulation software package [51], which includes both the geometrical description of the detector and the detector's response. An inclusive MC sample is produced at $E_{\rm cm} = 4.178$ GeV, which includes all open charm processes, initial state radiation (ISR) production of the $\psi(3770)$, $\psi(3686)$, and J/ψ, and $q\bar{q}(q = u, d, s)$ continuum processes, along with Bhabha scattering, $\mu^+\mu^-$, $\tau^+\tau^-$, and $\gamma\gamma$ events. The open charm processes are generated using ConExc [52]. The effects of ISR [53] and final state radiation (FSR) [54] are considered. The decay modes with known BF are generated using EvtGen [55] and the other modes are generated using LundCharm [56].

The ST D_s^- mesons are reconstructed from 14 hadronic decay modes, $D_s^- \to K^+K^-\pi^-$, $K^+K^-\pi^-\pi^0$, $K_S^0K^-$, $K_S^0K^-\pi^0$, $K_S^0K_S^0\pi^-$, $K_S^0K^+\pi^-\pi^-$, $K_S^0K^-\pi^+\pi^-$, $K^-\pi^+\pi^-$, $\pi^+\pi^-\pi^-$, $\eta_{\gamma\gamma}\pi^-$, $\eta_{\pi^0\pi^+\pi^-}\pi^-$, $\eta'_{\eta_{\gamma\gamma}\pi^+\pi^-}\pi^-$, $\eta'_{\gamma\rho^0}\pi^-$, and $\eta_{\gamma\gamma}\rho^-$, where the subscripts of $\eta^{(\prime)}$ represent the decay modes used to reconstruct $\eta^{(\prime)}$.

All charged tracks except for those from K_S^0 decays must originate from the interaction point (IP) with a distance of closest approach less than 1 cm in the transverse plane and less than 10 cm along the z axis. The polar angle θ of each track defined with respect to the positron beam must satisfy $|\cos\theta| < 0.93$. Measurements of the specific ionization energy loss (dE/dx) in the main drift chamber and the TOF are combined and used for particle identification (PID) by forming confidence levels for pion and kaon hypotheses (CL_π, CL_K). Kaon (pion) candidates are required to satisfy $CL_{K(\pi)} > CL_{\pi(K)}$.

To select K_S^0 candidates, pairs of oppositely charged tracks with distances of closest approach to the IP less than 20 cm along the z axis are assigned as $\pi^+\pi^-$ without PID requirements. These $\pi^+\pi^-$ combinations are required to have an invariant mass within ± 12 MeV of the nominal K_S^0 mass [57] and have a decay length of the reconstructed K_S^0 larger than 2σ of the vertex resolution away from the IP. The π^0 and η mesons are reconstructed via $\gamma\gamma$ decays. It is required that each electromagnetic shower starts within 700 ns of the event start time and its energy is greater than 25 (50) MeV in the barrel (end cap) region of the electromagnetic calorimeter (EMC) [47]. The opening angle between the shower and the nearest charged track has to be greater than 10°. The $\gamma\gamma$ combinations with an invariant mass $M_{\gamma\gamma} \in (0.115, 0.150)$ and $(0.50, 0.57)$ GeV/c^2 are regarded as π^0 and η mesons, respectively. A kinematic fit is performed to constrain $M_{\gamma\gamma}$ to the π^0 or η nominal mass [57]. The η candidates for the $\eta\pi^-$ ST channel are also reconstructed via $\pi^0\pi^+\pi^-$ candidates with an invariant mass within $(0.53, 0.57)$ GeV/c^2. The η' mesons are reconstructed via two decay modes, $\eta\pi^+\pi^-$ and $\gamma\rho^0$, whose invariant masses are required to be within (0.946,0.970) and $(0.940, 0.976)$ GeV/c^2, respectively. In addition, the minimum energy of the γ from $\eta' \to \gamma\rho^0$ decays must be greater than 0.1 GeV. The ρ^0 and ρ^+ mesons are reconstructed from $\pi^+\pi^-$ and $\pi^+\pi^0$ candidates, whose invariant masses are required to be larger than 0.5 GeV/c^2 and within $(0.67, 0.87)$ GeV/c^2, respectively.

The momentum of any pion not originating from a K_S^0, η, or η' decay is required to be greater than 0.1 GeV/c to reject soft pions from D^* decays. For $\pi^+\pi^-\pi^-$ and $K^-\pi^+\pi^-$ combinations, the dominant peaking backgrounds from $K_S^0\pi^-$ and $K_S^0K^-$ events are rejected by requiring the invariant mass of any $\pi^+\pi^-$ combination be more than ± 0.03 GeV/c^2 away from the nominal K_S^0 mass [57].

To suppress non-$D_s^+D_s^{*-}$ events, the beam-constrained mass of the ST D_s^- candidate

$$M_{\rm BC} \equiv \sqrt{(E_{\rm cm}/2)^2 - |\vec{p}_{D_s^-}|^2} \qquad (2)$$

is required to be within $(2.010, 2.073)$ GeV/c^2, where $\vec{p}_{D_s^-}$ is the momentum of the ST D_s^- candidate. This requirement retains D_s^- mesons directly from e^+e^- annihilation and indirectly from D_s^{*-} decay (See Fig. 1 in Ref. [58]). In each event, we only keep the candidate with the D_s^- recoil mass

$$M_{\rm rec} \equiv \sqrt{\left(E_{\rm cm} - \sqrt{|\vec{p}_{D_s^-}|^2 + m_{D_s^-}^2}\right)^2 - |\vec{p}_{D_s^-}|^2} \qquad (3)$$

closest to the nominal D_s^{*+} mass [57] per tag mode per charge. Figure 1 shows the invariant mass ($M_{\rm tag}$) spectra of the accepted ST candidates. The ST yield for each tag mode is obtained by a fit to the corresponding $M_{\rm tag}$ spectrum. The signal is described by the MC-simulated shape convolved with a Gaussian function representing the resolution difference between data and MC simulation. For the tag mode $D_s^- \to K_S^0K^-$, the peaking background from $D^- \to K_S^0\pi^-$ is described by the MC-simulated shape and then smeared with the same Gaussian function used in the signal shape with its size as a free parameter. The nonpeaking background is modeled by a second- or third-order Chebychev polynomial function. Studies of the inclusive MC sample validate this parametrization of the background shape. The fit results on these invariant mass spectra are shown in Fig. 1. The events in the signal regions are kept for further analysis. The total ST yield in data is $N_{\rm ST}^{\rm tot} = 388660 \pm 2592$ (see tag-dependent ST yields and background yields in the signal regions in Table I of Ref. [58]).

At the recoil sides of the ST D_s^- mesons, the $D_s^+ \to \mu^+\nu_\mu$ candidates are selected with the surviving neutral and

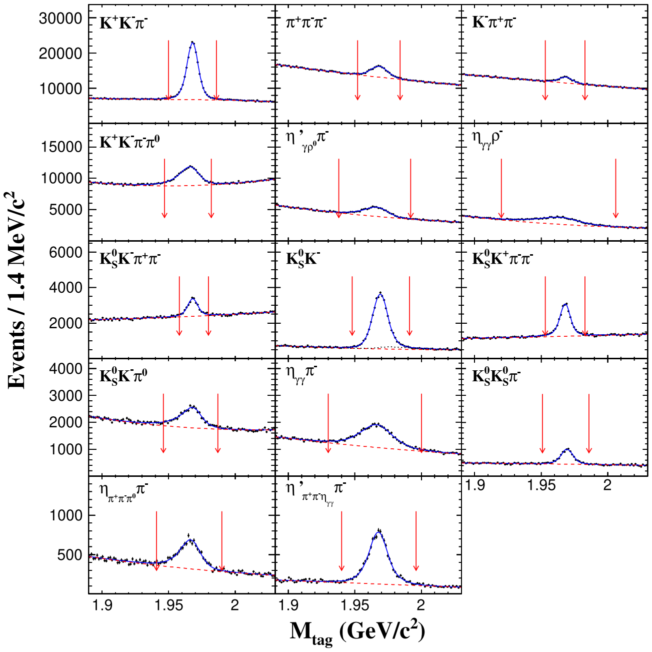

FIG. 1. Fits to the $M_{\rm tag}$ distributions of the accepted ST candidates. Dots with error bars are data. Blue solid curves are the fit results. Red dashed curves are the fitted backgrounds. The black dotted curve in the $K_S^0K^-$ mode is the $D^- \to K_S^0\pi^-$ component. The pairs of arrows denote the signal regions.

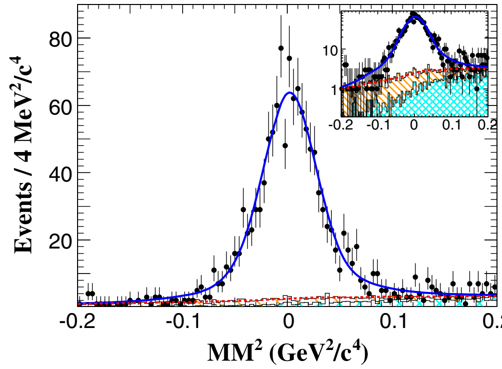

FIG. 2. Fit to the MM^2 distribution of the $D_s^+ \to \mu^+\nu_\mu$ candidates. Inset plot shows the same distribution in log scale. Dots with error bars are data. Blue solid curve is the fit result. Red dotted curve is the fitted background. Orange hatched and blue cross-hatched histograms are the BKGI component and the combined BKGII and BKGIII components, respectively (see text).

charged tracks. To select the soft $\gamma(\pi^0)$ from D_s^* and to separate signals from combinatorial backgrounds, we define two kinematic variables

$$\Delta E \equiv E_{\rm cm} - E_{\rm tag} - E_{\rm miss} - E_{\gamma(\pi^0)} \tag{4}$$

and

$$\mathrm{MM}^2 \equiv (E_{\rm cm} - E_{\rm tag} - E_{\gamma(\pi^0)} - E_\mu)^2 - |-\vec{p}_{\rm tag} - \vec{p}_{\gamma(\pi^0)} - \vec{p}_\mu|^2. \tag{5}$$

Here $E_{\rm miss} \equiv \sqrt{|\vec{p}_{\rm miss}|^2 + m^2_{D_s^+}}$ and $\vec{p}_{\rm miss} \equiv -\vec{p}_{\rm tag} - \vec{p}_{\gamma(\pi^0)}$ are the missing energy and momentum of the recoiling system of the soft $\gamma(\pi^0)$ and the ST D_s^-, where E_i and $\vec{p}_i$ [$i = \mu, \gamma(\pi^0)$ or tag] denote the energy and momentum of the muon, $\gamma(\pi^0)$ or ST D_s^-, respectively. MM^2 is the missing mass square of the undetectable neutrino. We loop over all remaining γ or π^0 candidates and choose the one giving a minimum $|\Delta E|$. The events with $\Delta E \in (-0.05, 0.10)$ GeV are accepted. The muon candidate is required to have an opposite charge to the ST D_s^- meson and a deposited energy in the EMC within (0.0,0.3) GeV. It must also satisfy a two dimensional (2D, e.g., $|\cos\theta_\mu|$ and momentum p_μ) requirement on the hit depth (d_μ) in the muon counter, as explained in Ref. [59]. To suppress the backgrounds with extra photon (s), the maximum energy of the unused showers in the DT selection ($E^{\rm max}_{{\rm extra}\gamma}$) is required to be less than 0.4 GeV and no additional charged track that satisfies the charged track selection criteria is allowed. To improve the MM^2 resolution, the candidate tracks, plus the missing neutrino, are subjected to a 4-constraint kinematic fit requiring energy and momentum conservation. In addition, the invariant masses of the two D_s mesons are constrained to the nominal D_s mass, the invariant mass of the $D_s^-\gamma(\pi^0)$ or $D_s^+\gamma(\pi^0)$ combination is constrained to the nominal D_s^* mass, and the combination with the smaller χ^2 is kept. Figure 2 shows the MM^2 distribution for the accepted DT candidate events.

To extract the DT yield, an unbinned constrained fit is performed to the MM^2 distribution. In the fit, the background events are classified into three categories: events with correctly reconstructed ST D_s^- and μ^+ but an unmatched $\gamma(\pi^0)$ from the D_s^{*-} (BKGI), events with a correctly reconstructed ST D_s^- but misidentified μ^+ (BKGII), and other events with a misreconstructed ST D_s^- (BKGIII). The signal and BKGI shapes are modeled with MC simulation. The signal shape is convolved with a Gaussian function with its mean and width as free parameters. The ratio of the signal yield over the BKGI yield is constrained to the value determined with the signal MC events. The size and shape of the BKGII and BKGIII components are fixed by analyzing the inclusive MC sample. From the fit to the MM^2 distribution, as shown in Fig. 2, we determine the number of $D_s^+ \to \mu^+\nu_\mu$ decays to be $N_{\rm DT} = 1135.9 \pm 33.1$.

The efficiencies for reconstructing the DT candidate events are determined with an exclusive MC sample of $e^+e^- \to D_s^+D_s^{*-}$, where the D_s^- decays to each tag mode and the D_s^+ decays to $\mu^+\nu_\mu$. Dividing them by the ST efficiencies determined with the inclusive MC sample yields the corresponding efficiencies of the $\gamma(\pi^0)\mu^+\nu_\mu$

reconstruction. The averaged efficiency of finding $\gamma(\pi^0)\mu^+\nu_\mu$ is $(52.67 \pm 0.19)\%$ as determined from

$$\varepsilon_{\gamma(\pi^0)\mu^+\nu_\mu} = f^{\rm cor}_{\mu{\rm PID}} \sum_i (N^i_{\rm ST}\varepsilon^i_{\rm DT})/(N^{\rm tot}_{\rm ST}\varepsilon^i_{\rm ST}), \qquad (6)$$

where $N^i_{\rm ST}$, $\varepsilon^i_{\rm ST}$, and $\varepsilon^i_{\rm DT}$ are the ST yield, ST efficiency, and DT efficiency in the ith ST mode, respectively. The factor $f^{\rm cor}_{\mu{\rm PID}} = 0.897$ accounts for the difference between the μ^+ PID efficiencies in data and MC simulation $[\varepsilon^{\rm data(MC)}_{\mu{\rm PID}}]$. These efficiencies are estimated using $e^+e^- \to \gamma\mu^+\mu^-$ samples but reweighted by the μ^+ 2D distribution of $D^+_s \to \mu^+\nu_\mu$. It is non-negligible mainly due to the imperfect simulation of d_μ and its applicability in different topology environments is verified via three aspects: (i) Studies with signal MC events show that $\varepsilon^{\rm MC}_{\mu{\rm PID}} = (74.79 \pm 0.03)\%$ for $D^+_s \to \mu^+\nu_\mu$ signals can be well reproduced by the 2D reweighted efficiency $\varepsilon^{\rm MC}_{\mu{\rm PID}} = (74.91 \pm 0.10)\%$ with $e^+e^- \to \gamma\mu^+\mu^-$ samples. (ii) Our nominal BF ($\mathcal{B}_{D^+_s\to\mu^+\nu_\mu}$) obtained later can be well reproduced by removing the d_μ requirement, with negligible difference but obviously lower precision due to much higher background [60]. (iii) The $\varepsilon^{\rm data(MC)}_{\mu{\rm PID}}$ for $e^+e^- \to \gamma_{\rm ISR}\psi(3686)$, $\psi(3686) \to \pi^+\pi^-J/\psi$, $J/\psi \to \mu^+\mu^-$ events can be well reproduced by the corresponding 2D reweighted efficiencies with $e^+e^- \to \gamma\mu^+\mu^-$ samples (see Table II of Ref. [58]). The BF of $D^+_s \to \mu^+\nu_\mu$ is then determined to be $(5.49 \pm 0.16_{\rm stat} \pm 0.15_{\rm syst}) \times 10^{-3}$ from

$$\mathcal{B}_{D^+_s\to\mu^+\nu_\mu} = f^{\rm rad}_{\rm cor} N_{\rm DT}/(N^{\rm tot}_{\rm ST}\varepsilon_{\gamma(\pi^0)\mu^+\nu_\mu}), \qquad (7)$$

where the radiative correction factor $f^{\rm rad}_{\rm cor} = 0.99$ is due to the contribution from $D^+_s \to \gamma\mathcal{D}^{*+}_s \to \gamma\mu^+\nu_\mu$ [61], with $\mathcal{D}^{*+}_s$ as a virtual vector or axial-vector meson. This contribution is almost identical with our signal process for low energy radiated photons. We further examine the BFs measured with individual tags which have very different background levels, and a good consistence is found (see Table I of Ref. [58] for tag-dependent DT yields, $\varepsilon_{\gamma(\pi^0)\mu^+\nu_\mu}$ and $\mathcal{B}_{D^+_s\to\mu^+\nu_\mu}$).

The systematic uncertainties in the BF measurement are estimated relative to the measured BF and are described below.

For uncertainties in the event selection criteria, the μ^+ tracking and PID efficiencies are studied with $e^+e^- \to \gamma\mu^+\mu^-$ events. After correcting the detection efficiency by $f^{\rm cor}_{\mu{\rm PID}}$, we assign 0.5% and 0.8% as the uncertainties in μ^+ tracking and PID efficiencies, respectively. The photon reconstruction efficiency has been previously studied with $J/\psi \to \pi^+\pi^-\pi^0$ decays [62]. The uncertainty of finding $\gamma(\pi^0)$ is weighted according to the BFs of $D^{*+}_s \to \gamma D^+_s$ and $D^{*+}_s \to \pi^0 D^+_s$ [57] and assigned to be 1.0%. The efficiencies for the requirements of $E^{\rm max}_{{\rm extra}\gamma}$ and no extra good charged track are studied with a DT hadronic sample. The systematic uncertainties are taken to be 0.3% and 0.9% considering the efficiency differences between data and MC simulation, respectively. The uncertainty of the ΔE requirement is estimated by varying the signal region by ± 0.01 GeV, and the maximum change of the BF, 0.5%, is taken as the systematic uncertainty.

To determine the uncertainty in the MM^2 fit, we change the fit range by ± 0.02 GeV$^2/c^4$, and the largest change of the BF is 0.6%. We change the signal shape by varying the $\gamma(\pi^0)$ match requirement and the maximum change is 0.2%. Two sources of uncertainty in the background estimation are considered. The effect of the background shape is obtained to be 0.2% by shifting the number of the main components of BKGII by $\pm 1\sigma$ of the uncertainties of the corresponding BFs [57], and varying the relative fraction of the main components of BKGII by 50%. The effect of the fixed number of the BKGII and BKGIII is estimated to be 0.5% by varying the nominal numbers by $\pm 1\sigma$ of their uncertainties. To evaluate the uncertainty in the fixed ratio of signal and BKGI, we perform an alternative fit to the MM^2 distribution of data without constraining the ratio of signal and BKGI. The change in the DT yield, 1.1%, is assigned as the relevant uncertainty.

The uncertainty in the number of ST D^-_s mesons is assigned to be 0.8% by examining the changes of the fit yields when varying the signal shape, background shape, bin size, and fit range and considering the background fluctuation in the fit. The uncertainty due to the limited MC size is 0.4%. The uncertainty in the imperfect simulation of the FSR effect is estimated as 0.4% by varying the amount of FSR photons in signal MC events [54]. The uncertainty due to the quoted BFs of D^{*-}_s subdecays from the Particle Data Group (PDG) [57] is examined by varying each subdecay BF by $\pm 1\sigma$. The efficiency change is found to be 0.4% and is taken as the associated uncertainty. The uncertainty in the radiative correction is assigned to be 1.0%, which is taken as 100% of its central value from theoretical calculation [61]. The ST efficiencies in the inclusive and signal MC samples are slightly different with each other due to different track multiplicities in these two environments. This may cause incomplete cancellation of the uncertainties of the ST efficiencies. The associated uncertainty is assigned as 0.6%, by taking into account the differences of the efficiencies of tracking/PID of $K^\pm$ and $\pi^\pm$, as well as the selections of neutral particles between data and MC simulation in different environments. The total systematic uncertainty is determined to be 2.7% by adding all the uncertainties in quadrature.

Combining our BF with the world average values of G_F, m_μ, $m_{D^+_s}$ and the lifetime of D^+_s [57] in Eq. (1) yields

$$f_{D^+_s}|V_{cs}| = 246.2 \pm 3.6_{\rm stat} \pm 3.5_{\rm syst}\ {\rm MeV}.$$

Here the systematic uncertainties arise mainly from the uncertainties in the measured BF (1.5%) and the lifetime of the D_s^+ (0.4%). Taking the CKM matrix element $|V_{cs}| = 0.97359^{+0.00010}_{-0.00011}$ from the global fit in the SM [57] or the averaged decay constant $f_{D_s^+} = 249.9 \pm 0.4$ MeV of recent LQCD calculations [8,10] as input, we determine

$$f_{D_s^+} = 252.9 \pm 3.7_{\rm stat} \pm 3.6_{\rm syst}\ {\rm MeV}$$

and

$$|V_{cs}| = 0.985 \pm 0.014_{\rm stat} \pm 0.014_{\rm syst}.$$

The additional systematic uncertainties according to the input parameters are negligible for $|V_{cs}|$ and 0.2% for $f_{D_s^+}$. The measured $|V_{cs}|$ is consistent with our measurements using $D \to \bar{K}\ell^+\nu_\ell$ [63–66] and $D_s^+ \to \eta^{(\prime)} e^+\nu_e$ [67], but with much better precision.

Combining the obtained $f_{D_s^+}|V_{cs}|$ and its counterpart $f_{D^+}|V_{cd}|$ measured in our previous work [68], along with $|V_{cd}/V_{cs}| = 0.23047 \pm 0.00045$ from the SM global fit [57], yields $f_{D_s^+}/f_{D^+} = 1.24 \pm 0.04_{\rm stat} \pm 0.02_{\rm syst}$. It is consistent with the CLEO measurement [2] within 1σ and the LQCD calculation within 2σ [8]. Alternatively, with the input of $f_{D_s^+}/f_{D^+} = 1.1749 \pm 0.0016$ calculated by LQCD [8], we obtain $|V_{cd}/V_{cs}|^2 = 0.048 \pm 0.003_{\rm stat} \pm 0.001_{\rm syst}$, which agrees with the one expected by $|V_{cs}|$ and $|V_{cd}|$ given by the CKMfitter within 2σ. Here, only the systematic uncertainty in the radiative correction is canceled since the two data samples were taken in different years.

Based on our result for $\mathcal{B}_{D_s^+\to\mu^+\nu_\mu}$ and those measured at the CLEO [2], *BABAR* [5], and Belle [6] experiments, along with a previous measurement at BESIII [7], the inverse-uncertainty weighted BF is determined to be $\bar{\mathcal{B}}_{D_s^+\to\mu^+\nu_\mu} = (5.49 \pm 0.17) \times 10^{-3}$ [69]. The ratio of $\bar{\mathcal{B}}_{D_s^+\to\mu^+\nu_\mu}$ over the PDG value of $\mathcal{B}_{D_s^+\to\tau^+\nu_\tau} = (5.48 \pm 0.23)\%$ [57] is determined to be $[(\mathcal{B}_{D_s^+\to\tau^+\nu_\tau})/(\bar{\mathcal{B}}_{D_s^+\to\mu^+\nu_\mu})] = 9.98 \pm 0.52$, which agrees with the SM predicted value of 9.74 within uncertainty.

The BFs of $D_s^+ \to \mu^+\nu_\mu$ and $D_s^- \to \mu^-\bar{\nu}_\mu$ decays are also measured separately. The results are $\mathcal{B}_{D_s^+\to\mu^+\nu_\mu} = (5.62 \pm 0.23_{\rm stat}) \times 10^{-3}$ and $\mathcal{B}_{D_s^-\to\mu^-\bar{\nu}_\mu} = (5.40 \pm 0.23_{\rm stat}) \times 10^{-3}$. The BF asymmetry is determined to be $A_{\rm CP} = [(\mathcal{B}_{D_s^+\to\mu^+\nu_\mu} - \mathcal{B}_{D_s^-\to\mu^-\bar{\nu}_\mu})/(\mathcal{B}_{D_s^+\to\mu^+\nu_\mu} + \mathcal{B}_{D_s^-\to\mu^-\bar{\nu}_\mu})] = (2.0 \pm 3.0_{\rm stat} \pm 1.2_{\rm syst})\%$, where the uncertainties in the tracking and PID efficiencies of the muon, the ST yields, the limited MC statistics, as well as the signal shape and fit range in MM^2 fits for D_s^+ and D_s^- have been studied separately and are not canceled.

In summary, by analyzing 3.19 fb^{-1} of e^+e^- collision data collected at $E_{\rm cm} = 4.178$ GeV with the BESIII detector, we have measured $\mathcal{B}(D_s^+ \to \mu^+\nu_\mu)$, the decay constant $f_{D_s^+}$, and the CKM matrix element $|V_{cs}|$. These are the most precise measurements to date, and are important to calibrate various theoretical calculations of $f_{D_s^+}$ and test the unitarity of the CKM matrix with better accuracy. We also search for LFU and *CP* violation in $D_s^+ \to \ell^+\nu_\ell$ decays, and no evidence is found.

The BESIII Collaboration thanks the staff of BEPCII and the IHEP computing center for their strong support. This work is supported in part by National Key Basic Research Program of China under Contract No. 2015CB856700; National Natural Science Foundation of China (NSFC) under Contracts No. 11235011, No. 11335008, No. 11425524, No. 11505034, No. 11575077, No. 11625523, No. 11635010, No. 11675200, and No. 11775230; the Chinese Academy of Sciences (CAS) Large-Scale Scientific Facility Program; the CAS Center for Excellence in Particle Physics (CCEPP); Joint Large-Scale Scientific Facility Funds of the NSFC and CAS under Contracts No. U1332201, No. U1532257, No. U1532258, and No. U1632109; CAS under Contracts No. KJCX2-YW-N29, No. KJCX2-YW-N45, No. QYZDJ-SSW-SLH003; 100 Talents Program of CAS; National 1000 Talents Program of China; INPAC and Shanghai Key Laboratory for Particle Physics and Cosmology; German Research Foundation DFG under Contracts No. Collaborative Research Center CRC 1044, FOR 2359; Istituto Nazionale di Fisica Nucleare, Italy; Koninklijke Nederlandse Akademie van Wetenschappen (KNAW) under Contract No. 530-4CDP03; Ministry of Development of Turkey under Contract No. DPT2006K-120470; National Science and Technology fund; The Swedish Research Council; U.S. Department of Energy under Contracts No. DE-FG02-05ER41374, No. DE-SC-0010118, No. DE-SC-0010504, and No. DE-SC-0012069; University of Groningen (RuG) and the Helmholtzzentrum fuer Schwerionenforschung GmbH (GSI), Darmstadt; WCU Program of National Research Foundation of Korea under Contract No. R32-2008-000-10155-0.

[a]Also at Bogazici University, 34342 Istanbul, Turkey
[b]Also at the Moscow Institute of Physics and Technology, Moscow 141700, Russia
[c]Also at the Functional Electronics Laboratory, Tomsk State University, Tomsk, 634050, Russia
[d]Also at the Novosibirsk State University, Novosibirsk, 630090, Russia
[e]Also at the NRC "Kurchatov Institute", PNPI, 188300, Gatchina, Russia
[f]Also at Istanbul Arel University, 34295 Istanbul, Turkey
[g]Also at Goethe University Frankfurt, 60323 Frankfurt am Main, Germany
[h]Also at Key Laboratory for Particle Physics, Astrophysics and Cosmology, Ministry of Education; Shanghai Key Laboratory for Particle Physics and Cosmology; Institute of Nuclear and Particle Physics, Shanghai 200240, People's Republic of China

[i]Also at Government College Women University, Sialkot - 51310. Punjab, Pakistan.
[j]Currently at: Center for Underground Physics, Institute for Basic Science, Daejeon 34126, Korea
[k]Also at Harvard University, Department of Physics, Cambridge, MA, 02138, USA

[1] D. Silverman and H. Yao, Phys. Rev. D **38**, 214 (1988).
[2] J. P. Alexander *et al.* (CLEO Collaboration), Phys. Rev. D **79**, 052001 (2009).
[3] P. Naik *et al.* (CLEO Collaboration), Phys. Rev. D **80**, 112004 (2009).
[4] P. U. E. Onyisi *et al.* (CLEO Collaboration), Phys. Rev. D **79**, 052002 (2009).
[5] P. del Amo Sanchez *et al.* (*BABAR* Collaboration), Phys. Rev. D **82**, 091103 (2010).
[6] A. Zupanc *et al.* (Belle Collaboration), J. High Energy Phys. 09 (2013) 139.
[7] M. Ablikim *et al.* (BESIII Collaboration), Phys. Rev. D **94**, 072004 (2016).
[8] A. Bazavov, C. Bernard, N. Brown, C. DeTar, A. X. El-Khadra, E. Gámiz, S. Gottlieb, U. M. Heller, J. Komijani, A. S. Kronfeld, J. Laiho, P. B. Mackenzie, E. T. Neil, J. N. Simone, R. L. Sugar, D. Toussaint, and R. S. Van de Water (Fermilab Lattice and MILC Collaborations), Phys. Rev. D **98**, 074512 (2018).
[9] A. Bazavov *et al.* (Fermilab Lattice and MILC Collaborations), Phys. Rev. D **90**, 074509 (2014).
[10] N. Carrasco, P. Dimopoulos, R. Frezzotti, P. Lami, V. Lubicz, F. Nazzaro, E. Picca, L. Riggio, G. C. Rossi, F. Sanfilippo, S. Simula, and C. Tarantino (ETM Collaboration), Phys. Rev. D **91**, 054507 (2015).
[11] P. A. Boyle, L. Del Debbio, A. Jüttner, A. Khamseh, F. Sanfilippo, and J. T. Tsang, J. High Energy Phys. 12 (2017) 008.
[12] Y. Yi-Bo *et al.*, Phys. Rev. D **92**, 034517 (2015).
[13] A. Bazavov *et al.* (Fermilab Lattice and MILC Collaborations), Phys. Rev. D **85**, 114506 (2012).
[14] C. T. H. Davies, C. McNeile, E. Follana, G. P. Lepage, H. Na, and J. Shigemitsu (HPQCD Collaboration), Phys. Rev. D **82**, 114504 (2010).
[15] H. Na, C. T. H. Davies, E. Follana, G. P. Lepage, and J. Shigemitsu (HPQCD Collaboration), Phys. Rev. D **86**, 054510 (2012).
[16] C. Aubin *et al.* (Fermilab Lattice and MILC Collaborations), Phys. Rev. Lett. **95**, 122002 (2005).
[17] E. Follana, C. T. H. Davies, G. P. Lepage, and J. Shigemitsu (HPQCD Collaboration), Phys. Rev. Lett. **100**, 062002 (2008).
[18] P. Dimopoulos *et al.* (ETM Collaboration), J. High Energy Phys. 01 (2012) 046.
[19] W. P. Chen, Y.-C. Chen, T.-W. Chiu, H.-Y. Chou, T.-S. Guu, and T.-H. Hsieh, Phys. Lett. B **736**, 231 (2014).
[20] Y. Namekawa, S. Aoki, K.-I. Ishikawa, N. Ishizuka, T. Izubuchi, K. Kanaya, Y. Kuramashi, M. Okawa, Y. Taniguchi, A. Ukawa, N. Ukita, and T. Yoshie (PACS-CS Collaboration), Phys. Rev. D **84**, 074505 (2011).
[21] A. Ali Khan, V. Braun, T. Burch, M. Göckeler, G. Lacagnina, A. Schäfer, and G. Schierholz (QCDSF Collaboration), Phys. Lett. B **652**, 150 (2007).
[22] T. W. Chiu, T.-H. Hsieh, J.-Y. Lee, P.-H. Liu, and H.-J. Chang, Phys. Lett. B **624**, 31 (2005).
[23] L. Lellouch and C.-J. David Lin (UKQCD Collaboration), Phys. Rev. D **64**, 094501 (2001).
[24] D. Becirevic, Ph. Boucaud, J. P. Leroy, V. Lubicz, G. Martinelli, F. Mescia, and F. Rapuano, Phys. Rev. D **60**, 074501 (1999).
[25] J. Bordes, J. Penarrocha, and K. Schilcher, J. High Energy Phys. 11 (2005) 014.
[26] S. Narison, arXiv:hep-ph/0202200.
[27] A. M. Badalian, B. L. B. Bakker, and Y. A. Simonov, Phys. Rev. D **75**, 116001 (2007).
[28] D. Ebert, R. N. Faustov, and V. O. Galkin, Phys. Lett. B **635**, 93 (2006).
[29] G. Cvetic, C. S. Kim, G.-L. Wang, and W. Namgung, Phys. Lett. B **596**, 84 (2004).
[30] H. M. Choi, Phys. Rev. D **75**, 073016 (2007).
[31] L. Salcedo, J. P. B. C. de Melo, D. Hadjmichef, and T. Frederico, Braz. J. Phys. **34**, 297 (2004).
[32] Z. G. Wang, W.-M. Yang, and S.-L. Wan, Nucl. Phys. **A744**, 156 (2004).
[33] J. F. Amundson, J. L. Rosner, M. A. Kelly, N. Horwitz, and S. L. Stone, Phys. Rev. D **47**, 3059 (1993).
[34] D. Becirevic, B. Blossier, A. Gérardin, A. Le Yaouanc, and F. Sanfilippo, Nucl. Phys. **B872**, 313 (2013).
[35] W. Lucha, D. Melikhov, and S. Simula, Phys. Lett. B **701**, 82 (2011).
[36] C. W. Hwang, Phys. Rev. D **81**, 054022 (2010).
[37] Z. G. Wang, Eur. Phys. J. C **75**, 427 (2015).
[38] J. P. Lees *et al.* (*BABAR* Collaboration), Phys. Rev. Lett. **109**, 101802 (2012).
[39] J. P. Lees *et al.* (*BABAR* Collaboration), Phys. Rev. D **88**, 072012 (2013).
[40] R. Aaij *et al.* (LHCb Collaboration), Phys. Rev. Lett. **115**, 111803 (2015).
[41] R. Aaij *et al.* (LHCb Collaboration), Phys. Rev. Lett. **113**, 151601 (2014).
[42] S. Wehle *et al.* (Belle Collaboration), Phys. Rev. Lett. **118**, 111801 (2017).
[43] S. Fajfer, I. Nisandzic, and U. Rojec, Phys. Rev. D **91**, 094009 (2015).
[44] G. C. Branco, P. M. Ferreira, L. Lavoura, M. N. Rebelo, M. Sher, and J. P. Silva, Phys. Rep. **516**, 1 (2012).
[45] G. C. Branco, R. G. Felipe, and F. R. Joaquim, Rev. Mod. Phys. **84**, 515 (2012).
[46] Charge-conjugate modes are always implied unless stated explicitly.
[47] M. Ablikim *et al.* (BESIII Collaboration), Nucl. Instrum. Methods Phys. Res., Sect. A **614**, 345 (2010).
[48] X. Li *et al.*, Radiat. Detect. Technol. Methods **1**, 13 (2017).
[49] Y. X. Guo *et al.*, Radiat. Detect. Technol. Methods **1**, 15 (2017).
[50] S. Agostinelli *et al.* (GEANT4 Collaboration), Nucl. Instrum. Methods Phys. Res., Sect. A **506**, 250 (2003).
[51] Z. Y. Deng *et al.*, Chin. Phys. C **30**, 371 (2006).
[52] R. G. Ping, Chin. Phys. C **38**, 083001 (2014).
[53] E. A. Kuraev and V. S. Fadin, Sov. J. Nucl. Phys. **41**, 466 (1985) Yad. Fiz. **41**, 733 (1985).

[54] E. Barberio and Z. Was, Comput. Phys. Commun. **79**, 291 (1994).

[55] D. J. Lange, Nucl. Instrum. Methods Phys. Res., Sect. A **462**, 152 (2001); R. G. Ping, Chin. Phys. C **32**, 599 (2008).

[56] J. C. Chen, G. S. Huang, X. R. Qi, D. H. Zhang, and Y. S. Zhu, Phys. Rev. D **62**, 034003 (2000).

[57] M. Tanabashi *et al.* (Particle Data Group), Phys. Rev. D **98**, 030001 (2018).

[58] See Supplemental Material at http://link.aps.org/supplemental/10.1103/PhysRevLett.122.071802 for the distributions of $M_{\rm BC}$, the ST yields and backgrounds in $M_{\rm tag}$ signal region, the DT yields, $\epsilon_{\gamma(\pi^0)\mu^+\nu_\mu}$ and $\mathcal{B}_{D_s^+\to\mu^+\nu_\mu}$ with different tags, and the validation of the correction of μ PID efficiency.

[59] The $|\cos\theta_{\mu,i}|$ is equally divided as $[0.2\times(i-1),$ $0.2\times i](i=1,2,3,4,$ or $5)$. In the first three $|\cos\theta_{\mu,i}|$ bins, we require d_μ greater than 17, $100\times p_\mu-(68+3\times i)$ and 33 cm for the muons with $p_\mu\le 0.85+0.03\times i$, $p_\mu\in(0.85+0.03\times i, 1.01+0.03\times i)$ and $p_\mu\ge 1.01+0.03\times i$, respectively. For other $|\cos\theta_{\mu,i}|$ bins, we require d_μ greater than 17 cm uniformly.

[60] Without the d_μ requirement, there will be higher background from $D_s^+\to\tau^+\nu_\tau, \tau^+\to\pi^+\bar{\nu}_\tau$.

[61] G. Burdman, T. Goldman, and D. Wyler, Phys. Rev. D **51**, 111 (1995).

[62] M. Ablikim *et al.* (BESIII Collaboration), Phys. Rev. D **83**, 112005 (2011).

[63] M. Ablikim *et al.* (BESIII Collaboration), Phys. Rev. D **92**, 072012 (2015).

[64] M. Ablikim *et al.* (BESIII Collaboration), Phys. Rev. D **96**, 012002 (2017).

[65] M. Ablikim *et al.* (BESIII Collaboration), Phys. Rev. D **92**, 112008 (2015).

[66] M. Ablikim *et al.* (BESIII Collaboration), Phys. Rev. Lett. **122**, 011804 (2019).

[67] M. Ablikim *et al.* (BESIII Collaboration), arXiv:1901.02133.

[68] M. Ablikim *et al.* (BESIII Collaboration), Phys. Rev. D **89**, 051104 (2014).

[69] To be consistent with results at CLEO and BESIII, the BFs measured by Belle and *BABAR* have been further corrected by $f^{\rm rad}_{\rm cor}$. The uncertainty in $f^{\rm rad}_{\rm cor}$ is common for individual measurements, but will be taken into account in the averaged BF. For the previous measurement in BESIII, we quote the BF without the LFU constraint.